DOI: 10.1002/cmdc.201100060

Synthesis, Structural Characterization, and Pro-apoptotic Activity of 1-Indanone Thiosemicarbazone Platinum(II) and Palladium(II) Complexes: Potential as Antileukemic Agents

Natalia Gómez,[a] Diego Santos,[b] Ramiro Vázquez,[a] Leopoldo Suescun,[c] Álvaro Mombrú,[c] Monica Vermeulen,[e] Liliana Finkielsztein,[a] Carina Shayo,[d] Albertina Moglioni,*[a] Dinorah Gambino,*[b] and Carlos Davio*[a]

In the search for alternative chemotherapeutic strategies against leukemia, various 1-indanone thiosemicarbazones, as well as eight novel platinum(II) and palladium(II) complexes, with the formula $[MCl_2(HL)]$ and [M(HL)(L)]Cl, derived from two 1-indanone thiosemicarbazones were synthesized and tested for antiproliferative activity against the human leukemia U937 cell line. The crystal structure of $[Pt(HL1)(L1)]Cl\cdot 2MeOH$, where L1 = 1-indanone thiosemicarbazone, was solved by X-ray diffraction. Free thiosemicarbazone ligands showed no antiproliferative effect, but the corresponding platinum(II) and palladium(II) complexes inhibited cell proliferation and induced apoptosis. Platinum(II) complexes also displayed selective apoptotic activity in U937 cells but not in peripheral blood monocytes or the human hepatocellular carcinoma HepG2 cell line used to screen for potential hepatotoxicity. Present findings show that, in U937 cells, 1-indanone thiosemicarbazones coordinated to palladium(II) were more cytotoxic than those complexed with platinum(II), although the latter were found to be more selective for leukemic cells suggesting that they are promising compounds with potential therapeutic application against hematological malignancies.

Introduction

Acute leukemia is a malignant neoplasm of the hematopoietic cells characterized by an abnormal proliferation of precursor cells, decreased rate of apoptosis, and arrest in cell differentiation. Unfortunately, most leukemia turn refractory to chemotherapy necessitating the development of alternative chemotherapeutic strategies.[1] Due to the nature of leukemic processes, chemotherapy constitute an important tool in the fight against such hematological malignancies, although most of the currently used drugs display significant toxicity and are often nonspecific. In addition, development of drug resistance, severe side effects, and a reduced spectrum of tumors against which they are active also limit the clinical utility of these established drugs. Over the years, the identification of new, effective chemotherapeutics against leukemia has remained a focus of intense interest. In this regard, to develop highly effective, selective anticancer drugs is a major challenge, particularly if the cancer is resistant to established therapies. Nowadays, many of the therapeutic agents used in the treatment of malignant neoplasms, including VP16, cisplatin, adriamycin, and taxol, exert their anticancer effects by inducing apoptosis.[2] In fact, a challenging goal of new chemotherapeutic agents is to promote apoptosis in cancer cells, while shielding normal cells.

Thiosemicarbazones (TSCs) are compounds of considerable interest because of their important chemical properties and potentially beneficial biological activities. In recent years, a large number of TSCs with diverse biological properties, including antibacterial, antiviral, antimycotic and antitumor activity, has been described.[3–7] TSCs contain a rich set of donor atoms and are well-known metal ion chelators. In fact, many of the biological responses induced by TSCs depend on their metal complexation.[7] The antitumor activity of TSCs is attrib-

[a] N. Gómez, R. Vázquez, Prof. Dr. L. Finkielsztein, Prof. Dr. A. Moglioni, Prof. Dr. C. Davio
Cátedra de Química Medicinal, Facultad de Farmacia y Bioquímica
Universidad de Buenos Aires
Junin 956, C1113AAD, Buenos Aires (Argentina)
Fax: (+54)-11-4786-2564
E-mail: cardavio@ffyb.uba.ar
amoglio@ffyb.uba.ar

[b] D. Santos, Prof. Dr. D. Gambino
Cátedra de Química Inorgánica, Departamento Estrella Campos
Facultad de Química, Universidad de la República
Avda General Flores 2124, 11800 Montevideo (Uruguay)
Fax: (+598)-292-41906
E-mail: dgambino@fq.edu.uy

[c] L. Suescun, Á. Mombrú
Crystallography, Solid State and Materials Laboratory
DETEMA, Facultad de Química, Universidad de la República
Avda General Flores 2124, CC 1157, 11800 Montevideo (Uruguay)

[d] Dr. C. Shayo
Laboratorio de Farmacología y Patología Molecular
Instituto de Biología y Medicina Experimental (IBYME)-CONICET
Vuelta de Obligado 2490, C1428ADN Buenos Aires (Argentina)

[e] Dr. M. Vermeulen
Departamento de Inmunología, Instituto de Investigaciones Hematológicas
Academia Nacional de Medicina
Pacheco de Melo 3081, Buenos Aires (Argentina)

Supporting information for this article is available on the WWW under http://dx.doi.org/10.1002/cmdc.201100060.

uted to their ability to form chelates leading to compounds that can redox cycle, which results in reactive oxygen species (ROS) generation and marked chelation. It has been described that these compounds not only target ribonucleotide reductase, but also other intracellular molecules such as N-myc downstream-regulated gene-1 (NDRG1) and DNA topoisomerase IIα (top2α).[8] Furthermore, since neoplastic cells require a higher amount of essential metals for proliferation than normal cells, metal chelation becomes an interesting strategy when developing anticancer drugs.[9] Therefore, given their ability to form chelates, TSCs are structures of particular pharmaceutical interest for the development of potential therapeutic agents. In point of fact, 3-aminopyridine-2-carboxaldehyde thiosemicarbazone (triapine) is currently being evaluated in human phase II clinical trials as an anticancer agent.[10,11] The chemical nature of active TSCs reported in the literature is diverse. The imine moiety is typically substituted at the carbon atom with aromatic, aliphatic and α-N-heterocyclic groups.[8,12–14] Furthermore, given the ability of these compounds to form chelates, their complexation with metals, such as Ni, Cu, Fe, Co, Ru, Pd and Pt, has been used as a strategy to achieve derivatives with enhanced biological activity. Some examples are nickle(II) complexes of *S*-citronellalthiosemicarbazone,[15] copper(II) complexes of 2-acetylpyridine-4,4-dimethyl-3-TSC and di-2-pyridylketone-4,4-dimethyl-3-TSC,[16] antimony-(III) complexes of 2-benzoylpyridine-TSC,[17] and platinum(II) and palladium(II) complexes of 5-nitrofuran-TSC derivatives.[18–20] Coordination of TSCs with metals has been shown to enhance their biological activity and even make them display a particular activity not shown by the free ligand. It has been proposed that this results from increased TSCs lipophilicity, which would favor entry into the cell.[21]

The present study reports the synthesis, and characterization of 1-indanone-derived TSCs (**1**–**10**), as well as platinum(II) and palladium(II) complexes of two of these TSCs (**1** and **8**) with the formula $[MCl_2(HL)]$ and [M(HL)(L)]Cl (**11**–**18**). The biological activity of all compounds was assessed in the human leukemia U937 cell line. The effect of substituents on the TSC moiety and metal complexation were simultaneously addressed regarding the potential antileukemic response. Results showed that the free ligands had no effect on U937 cells growth, whereas the platinum(II) and palladium(II) complexes inhibited cell proliferation and induced apoptosis. In particular, the platinum(II) complexes exhibited selective cytotoxicity in U937 cells over peripheral blood monocytes or HepG2 cells.<

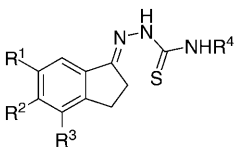

1: R^1 = H, R^2 = H, R^3 = H, R^4 = H
2: R^1 = H, R^2 = H, R^3 = Me, R^4 = H
3: R^1 = H, R^2 = Me, R^3 = H, R^4 = H
4: R^1 = OMe, R^2 = H, R^3 = H, R^4 = H
5: R^1 = H, R^2 = OMe, R^3 = H, R^4 = H
6: R^1 = H, R^2 = H, R^3 = OMe, R^4 = H
7: R^1 = H , R^2 = OMe, R^3 = OMe, R^4 = H
8: R^1 = OMe, R^2 = OMe, R^3 = H , R^4 = H
9: R^1 = H, R^2 = OMe, R^3 = H, R^4 = Allyl
10: R^1 = H, R^2 = H, R^3 = OMe, R^4 = Allyl

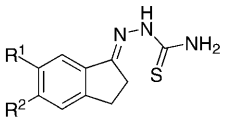

HL1 (**1**): R^1 = R^2 = H
HL2 (**8**): R^1 = R^2 = OMe

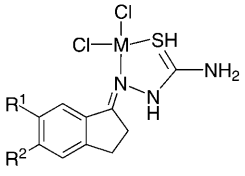

M = Pd or Pt

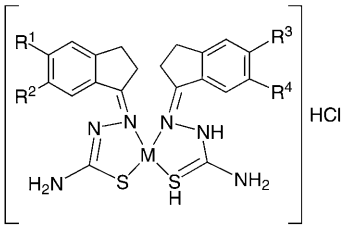

[$PtCl_2$(HL1)] **11**
[$PtCl_2$(HL2)] **12**
[$PdCl_2$(HL1)] **15**
[$PdCl_2$(HL2)] **16**

[Pt(HL1)(L1)]Cl **13**
[Pt(HL2)(L2)]Cl **14**
[Pd(HL1)(L1)]Cl **17**
[Pd(HL2)(L2)]Cl **18**

Results and Discussion

Synthesis and spectroscopy

Modification of the TSC structure allows the synthesis of novel compounds to explore their biological activities. In the present study, we adopted three approaches to obtain different TSCs derivatives. The TSC structure was modified at the indanone (R^1, R^2 and R^3), at N4 (R^4), and by chelation with platinum(II) or palladium(II). We previously reported the synthesis and chemical characterization of various TSCs (**1**–**8**) with modifications at the indanone structure;[5] TSCs **9** and **10**, bearing an allyl group at the N4 of the TSC moiety, were synthesized using the same method.

Coordination of TSCs with metals has been shown to enhance their biological activity. In the present study, two different TSCs were coordinated to platinum(II) and palladium(II). Compounds **1** and **8** were chosen for metal coordination, the former due to its simple structure without substituents and the latter for its more complex structure bearing substituents R^1 and R^2 on the indanone skeleton. Complexes were obtained by reaction of $Na_2[PdCl_4]$ or $K_2[PtCl_4]$, with compounds **1** (HL1) and **8** (HL2), rendering four palladium(II) and four platinum(II) compounds (**11**–**18**). Complexes with the formula $[MCl_2(HL)]$ (**11**, **12**, **15**, **16**) were synthesized using a metal/ligand molar ratio of 1:1. Complexes with the formula [M(HL)(L)]Cl (**13**, **14**, **17**, **18**) were obtained by using a metal/ligand molar ratio of 1:2. Analytical data were consistent with the proposed formulae (see Experimental Section).

$[MCl_2(HL)]$ complexes were nonconducting compounds, whereas [M(HL)(L)]Cl compounds were 1:1 electrolytes. Thermogravimetric analysis (TGA) of [Pt(HL1)(L1)]Cl isolated powder released one methanol solvation molecule per molecule of complex beginning at around 30 °C and centered at 70 °C (mass release for [Pt(HL1)(L1)]Cl·CH_3OH (%): calculated: 4.8, found: 5.0). Mass release of the analogous Pt-L2 complex was consistent with the formula [Pt(HL2)(L2)]Cl·$2H_2O$ (mass release for [Pt(HL2)(L2)]Cl·$2H_2O$ (%): calculated: 4.5, found: 4.5). TGA results for the palladium(II) compounds agreed with similar formulae, [Pd(HL1)(L1)]Cl·CH_3OH and [Pd(HL2)(L2)]Cl·$2H_2O$, showing that platinum(II) replacement by palladium(II) led to analo-

gous compounds. Mass spectra of complexes showing slight solubility in methanol, ([M(HL)(L)]Cl), exhibited a peak assigned to the molecular ion whose *m/z* value matched with the expected theoretical value. In addition, experimental isotopic patterns matched up with the expected patterns for the proposed formulae. Unfortunately, no suitable spectra for the other complexes were achieved due to their extremely poor solubility in methanol. Single crystals of [Pt(HL1)(L1)]Cl·2CH_3OH (**13**) were obtained by slow evaporation of the reaction medium. Crystals lost one methanol solvation molecule very slowly leading to the monosolvated complex, as confirmed by elemental analysis.

Fourier transform infrared spectroscopy showed significant vibration bands for the metal complexes. These were used to tentatively assign the ligand coordination mode. After coordination, the $\nu_{(C=N)}$ bands of TSC free ligands (HL1: 1599 cm^{-1}, HL2: 1595 cm^{-1}) shifted to higher frequencies. In addition, $\nu_{(C=S)}$ bands, at approximately 825–855 cm^{-1}, shifted to lower frequencies. These changes are consistent with bidentate coordination of the TSC ligands through the thiocarbonylic sulfur and the azomethynic nitrogen.[22–25] The $\nu_{(NH)}$ band at ~3155 cm^{-1} was present in all [MCl_2(HL)] complexes, supporting the hypothesis that the ligand is not deprotonated.

Crystal structure of *cis*-[Pt(HL1)(L1)]Cl·2MeOH

cis-[Pt(HL1)(L1)]Cl·2MeOH (**13**) crystals consist of cationic units of *cis*-[Pt(HL1)(L1)]$^+$ showing atypical *cis* configuration of HL1 and L1 ligands in a distorted square-planar configuration of N- and S-coordinated atoms around the platinum(II) center (Figure 1). The Pt–N and Pt–S bond distances (Table 1) corresponded to those reported for the only *cis*-platinum(II) complex found in the literature[26] showing Pt–N and Pt–S bond distances of 2.060 and 2.268 Å, respectively. The distortion from planar coordination polyhedra might be caused by the twisting of the Pt–N bonds above and below the S–Pt–S plane due to the *cis* configuration of the ligands. The five-membered Pt–N–N–C–S rings show an envelope configuration with platinum(II) occupying the out-of-plane position, deviating about 0.8 Å from the N–N–C–S plane. The main difference between both ligands is the bond lengths and angles, including N(12) and N(22) atoms in HL1 and L1 ligands, respectively (Table 1). It results from N(22) protonation that makes this atom exhibit sp^2 hybridization with N(21)–N(22)–C(21) angle of 118.7(11)°, whereas negatively charged N(12) shows sp^3 hybridization with N(11)–N(12)–C(11) bond angle of 111.4(9)°. Although hydrogen atoms failed to be identified in the difference electron density maps, the protonated ligand was easily identified by inspection of the mentioned bond distances and angles. The tails of the ligands were located in parallel but their aromatic rings were far apart suggesting an absence of a π–π interaction between them. Charge balance in the crystal was achieved by the presence of a chlorine counterion located close to the protonated HL1 ligand forming hydrogen bonds with hydrogen atoms linked to N21 and N22. Two labile crystallization methanol molecules completed the crystal structure, filling the void left by the absence of ligand tails at one side of the platinum(II) ion. These two molecules were connected to Cl(1), N(13) and N(23) by hydrogen bonds completing a full network of low-energy interactions. The infrared spectra of these complexes resulted as expected for their proposed structure according to our previously reported work.[22]

Table 1. Selected bond distances and bond angles for compound **13**.[a]

Bond	Distance [Å]	Bond	Angle [°]
Ligand 1			
Pt(1)–N(11)	2.044(9)	N(11)–Pt(1)–N(21)	99.8(4)
Pt(1)–S(11)	2.259(3)	N(11)–Pt(1)–S(21)	173.2(2)
S(11)–C(11)	1.751(11)	N(11)–Pt(1)–S(11)	80.9(2)
C(11)–N(12)	1.307(14)	Pt(1)–S(11)–C(11)	94.8(4)
C(11)–N(13)	1.347(15)	S(11)–C(11)–N(12)	124.0(9)
N(11)–N(12)	1.383(12)	C(11)–N(12)–N(11)	111.4(9)
N(11)–C(12)	1.311(13)	N(12)–N(11)–Pt(1)	118.0(6)
Ligand 2			
Pt(1)–N(21)	2.075(11)	S(11)–Pt(1)–S(21)	97.04(12)
Pt(1)–S(21)	2.287(3)	N(21)–Pt(1)–S(11)	175.5(2)
S(21)–C(21)	1.723(15)	N(21)–Pt(1)–S(21)	82.8(3)
C(21)–N(22)	1.316(18)	Pt(1)–S(11)–C(11)	95.1(5)
C(21)–N(23)	1.309(16)	S(11)–C(11)–N(12)	121.0(10)
N(21)–N(22)	1.401(13)	C(11)–N(12)–N(11)	118.7(11)
N(21)–C(22)	1.293(16)	N(12)–N(11)–Pt(1)	111.2(7)

[a] Values in parentheses represent the estimated standard deviations in the last significant figure. CCDC-778905 contains the supplementary crystallographic data for this paper. These data can be obtained free of charge from The Cambridge Crystallographic Data Centre (CCDC) via www.ccdc.cam.ac.uk.

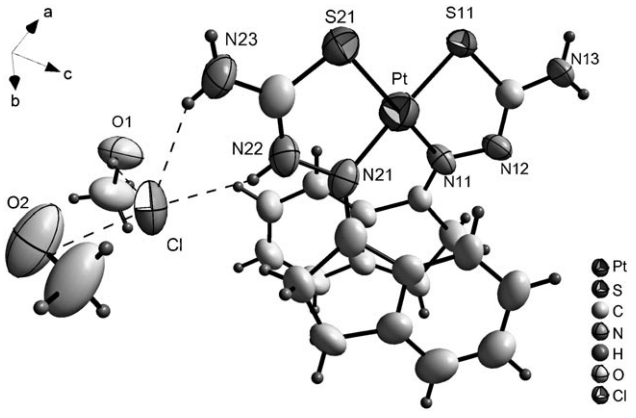

Figure 1. X-ray crystal structure of *cis*-[Pt(H**L1**)(**L1**)]Cl·2MeOH (**13**). Thermal ellipsoids are plotted at 30% probability levels and hydrogen atoms are omitted for clarity. CCDC-778905 contains the supplementary crystallographic data for this paper. These data can be obtained free of charge from The Cambridge Crystallographic Data Centre (CCDC) via www.ccdc.cam.ac.uk.

Antiproliferative activity

The antiproliferative and cytotoxic effects of TSCs were evaluated in U937 cells (Table 2). Free ligands **1**–**10** showed neither antiproliferative nor cytotoxic activity in the range of concentrations studied. Due to their low water solubility, concentrations higher than 50 μM could not be tested. Previous studies from our laboratory showed that compounds of this nature

Table 2. Inhibition of cell proliferation (IC_{50}) and cytotoxic activity (CC_{50}) of the 1-indanone thiosemicarbazones and their platinum(II) and palladium(II) complexes.

Compd	IC_{50} [μM][a]	CC_{50} [μM][b]
1–**10**	>50	>50
11	26.86 (22.05–32.70)	35.89 (30.72–41.92)
12	23.67 (15.88–35.28)	23.31 (18.35–29.60)
13	21.41 (16.55–27.70)	16.81 (12.95–21.82)
14	17.79 (16.16–19.60)	24.12 (19.48–29.87)
15	0.2257 (0.1926–0.2645)	0.2331 (0.1539–0.3531)
16	0.1817 (0.1037–0.3184)	0.2803 (0.2349–0.3346)
17	0.1452 (0.1206–0.1748)	0.1132 (0.08698–0.1474)
18	0.1542 (0.1312–0.1812)	0.1297 (0.08525–0.1972)
$K_2[PtCl_4]$	>50	>50
$Na_2[PdCl_4]$	>1	>1
Cisplatin	8.081 (7.266–8.987)	13.39 (12.80–14.02)

[a] IC_{50} values were determined by measuring [^{3}H]thymidine incorporation following 48 h exposure to different concentrations of the compounds in U937 cells. [b] CC_{50} values were assessed by Trypan Blue dye exclusion assays. Further details on these assays are given in the Experimental Section. Data represent the mean of three independent experiments; the 95% confidence interval is given in parentheses.

tend to form aggregates in water irrespective of the substituent at the N4 position (hydrogen or allyl group).[27] Current findings show that changes to the indanone substituents (R^1, R^2 and R^3) or the N4 substituents on the TSC moiety fail to induce antiproliferative activity. Conversely, platinum(II) and palladium(II) complexes **11**–**18** derived from compounds **1** and **8**, showed significant antiproliferative and cytotoxic activity in this cell line. Moreover, the cytotoxic activity of platinum(II) complexes was comparable to that of cisplatin, an established anticancer drug, while palladium(II) complexes resulted more potent than the latter.

Although palladium(II) TSC complexes have been reported to exhibit comparable or slightly greater cytotoxicity than analogous platinum(II) compounds,[21] in the present study, palladium(II) complexes (**15**–**18**) were found to be 100-fold more potent than their corresponding platinum(II) analogues (**11**–**14**) (see Table 2). Platinum(II) and palladium(II) complexes with bidentate N,S-chelating ligands show high thermodynamic stability. Nevertheless, platinum(II) compounds show high kinetic inertness towards ligand substitution, whereas those of palladium(II) are kinetically labile. It has been proposed that the high thermodynamic stability and high kinetic lability of palladium(II) complexes make them more suitable to interact with cancer cells.[21] Neither $K_2[PtCl_4]$ nor $Na_2[PdCl_4]$ showed antiproliferative or cytotoxic activity, supporting the hypothesis that the effect on cell proliferation and viability exhibited by compounds **11**–**18** is not due to the metal itself, but to their complexed species.

Proapoptotic activity

The close IC_{50} and CC_{50} values for compound **11**–**18** suggest that inhibition of cell proliferation could be ascribed to cell death or loss of cell viability. Actually cell death is an important variable not only in cancer development but also in cancer prevention and therapy. The major approach for cancer treatment is the removal of the neoplasm and/or the induction of cancer cells death by radiation, chemotherapy, antibodies or immune system cells.[28] Cytotoxic agents induce cell death by necrosis or apoptosis. Apoptosis is a controlled type of cell death induced by a variety of physiological and pharmacological stimuli. The number of leukemia cells in a patient could be reduced by either inhibiting cell proliferation or inducing cell death. In vitro studies with tumor and leukemia cell lines report that the cytotoxic drugs used in chemotherapy induce cell death through the activation of diverse apoptotic signaling pathways.[29]

Increased release of lactate dehidrogenase (LDH) from cells supports impairment of plasma membrane permeability resulting from the loss of cell viability. Therefore, LDH activity was measured in the medium following 24 h exposure to the different compounds. Results showed that LDH activity increased in the supernatant of cells treated with compounds **11**–**18** at their EC_{50} value (20 μM compounds **11**–**14** and 0.3 μM compounds **15**–**18**; Figure 2a). Conversely, no changes in LDH activity were observed when cells were exposed to compounds **1** and **8** (50 μM) or the tetrachlorometallates (20 μM $K_2[PtCl_4]$ and 0.3 μM $Na_2[PdCl_4]$). These findings show that palladium(II) complexes display higher cytotoxic activity than platinum(II) complexes. As impaired membrane permeability may be caused by necrosis or programmed cell death, apoptosis was evaluated in cells following incubation with the different compounds for 24 h.

Cleavage and activation of caspase 3, which is the key terminal effector of apoptosis, was assessed by Western blot analysis. Following U937 cells exposure to IC_{50} level of compounds **11**–**18**, the cleavage of pro-caspase 3 was observed (Figure 2b). Furthermore the cleavage of caspase 3 downstream substrate and mediator of cell death, poly(ADP-ribose)polymerase (PARP), was also evidenced following 24 h exposure to compounds **11**–**18** (Figure 2b). These findings clearly support that the compounds induce caspase 3 activation. Therefore, the enzyme activity was measured. Figure 2c illustrates that an increase in caspase 3 activity occurred in the presence of the different compounds except for the free ligands **1** and **8** or $K_2[PtCl_4]$ and $Na_2[PdCl_4]$.

Induction of apoptosis was also assessed in cells exposed for 24 h to compounds **11**–**18**, $K_2[PtCl_4]$ and $Na_2[PdCl_4]$ using the annexin–fluorescein isothiocyanate (FITC) assay kit (Figure 3). In this assay, the placental protein annexin V (AnV) binds to phosphatidylserine (PS) residues in the presence of Ca^{2+}. In viable cells, PS is located in the plasma membrane facing the cytosol and is therefore unable to bind AnV, whereas in apoptotic cells, PS residues are enzymatically flipped to the outer layer of the membrane ready to bind AnV. On the other hand, costaining with propidium iodide (PI), which binds to DNA and penetrates cells only when membrane permeability is impaired, permits the identification of early- and late-stage apoptotic cells, as well as necrotic cells, where the latter is positive for PI staining but negative for AnV-FITC labeling. Untreated cells exhibited low PI and AnV staining, with approximately 92% viable cells. However, cells exposed to compounds **11**–**18**

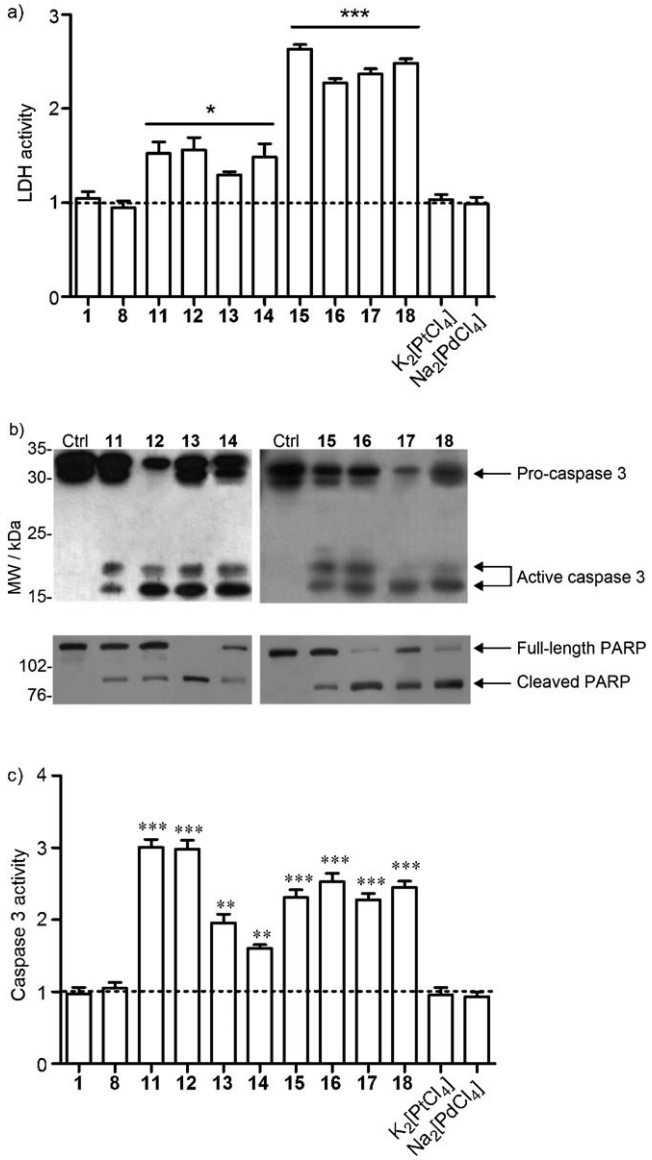

Figure 2. Apoptotic activity in the U937 cell line. Cells were treated for 24 h with: **1** and **8** (50 μM), **11**–**14** and $K_2[PtCl_4]$ (20 μM), and **15**–**18** and $Na_2[PdCl_4]$ (0.3 μM). After treatment, the cells were further analyzed as detailed in the Experimental Section. a) LDH activity is given with respect to control cells (-----). b) Determination of cleaved caspase 3 and PARP by Western blot analysis. U937 cells were treated and harvested, and equal amounts of protein were subjected to SDS-PAGE and analyzed by Western blot with anti-caspase 3 and PARP antibodies. Data are representative of at least three independent experiments. c) Casapase 3 activity is given with respect to control cells (-----). The data given in panels a and c represent the mean ± SEM ($n=3$): (*) $p<0.05$; (**) $p<0.01$ and (***) $p<0.001$.

showed a significant increase in PI and AnV staining, with an elevated number of cells in the early (An^+PI^-) and late (An^+PI^+) stages of apoptosis. On the other hand, cells exposed to $K_2[PtCl_4]$ and $Na_2[PdCl_4]$ alone showed no difference with untreated cells.

These results, together with the observation that the tetrachlorometallate salts failed to inhibit cell proliferation and exhibited no cytotoxicity at the concentration tested, suggest that TSC metal coordination is responsible for the activity displayed by the complexes. Furthermore, the present findings indicate that palladium(II) complexes exhibit higher cytotoxicity through apoptosis induction in leukemic cells than the platinum(II) complexes. The experimental observation that the free ligands and the tetrachlorometallate salts failed to induce apoptosis strongly support that the activity results from the structural nature of the complexes.

Although palladium(II) analogues related to cisplatin and its derivatives showed higher toxicity and lower activity, attributed to the high lability of palladium(II) compounds, there are several examples in the literature of palladium(II) compounds showing higher activities than their platinum(II) analogues, particularly with thiosemicarbazones as ligands.[18–20, 26, 30] Nevertheless, in many cases, palladium(II) compounds are more toxic than the isostructural platinum(II) compounds; again, this is due to the higher lability of palladium(II) compared with platinum(II). Therefore, we considered the observed selectivity to be worthy of further scrutiny.

Selectivity

Specific induction of apoptosis in cancer cells is one of the major goals in anticancer strategies because indiscriminate apoptosis activation may result harmful to healthy tissue and can induce the development of new tumors.[31] In order to evaluate the selectivity of active compounds **11**–**18**, peripheral blood monocytes were used and results compared to those obtained in U937 cells.

LDH release was measured in peripheral blood monocytes following incubation for 24 h with compounds **11**–**18** at the concentrations previously used to assess their pro-apoptotic response in U937 cells. A significant increase in LDH was observed in peripheral blood monocytes treated with palladium(II) complexes **15**–**18**, whereas no changes were observed in the enzyme activity when cells were exposed to platinum(II) compounds (Figure 4a). Furthermore, palladium(II) complexes also increased caspase 3 activity in peripheral blood monocytes, and the AnV/PI staining profile showed cells undergoing early and late stages of apoptosis (Figure 4b and c). These findings strongly support the hypothesis that platinum(II) complexes are more selective towards U937 cells than palladium(II) complexes.

In an attempt to evaluate potential hepatotoxicity of the active compounds (**11**–**18**), their effect was tested in HepG2 cells, a human hepatocellular carcinoma cell line used to estimate xenobiotic hepatoxicity because of its close functional resemblance to adult hepatocytes.[32] Active compounds failed to induce cytotoxicity in HepG2 cells. Apoptosis was not induced by platinum(II) complexes but cell exposure to palladium(II) complexes increased the rate of cells undergoing the early stages of apoptosis (Figure 4a–c). These findings suggest that platinum(II) complexes would not be cytotoxic and further supports the observation that they are selective for U937 cells.

Conclusions

The present study is, to our knowledge, the first to show that platinum(II) complexes derived from 1-indanone thiosemicar-

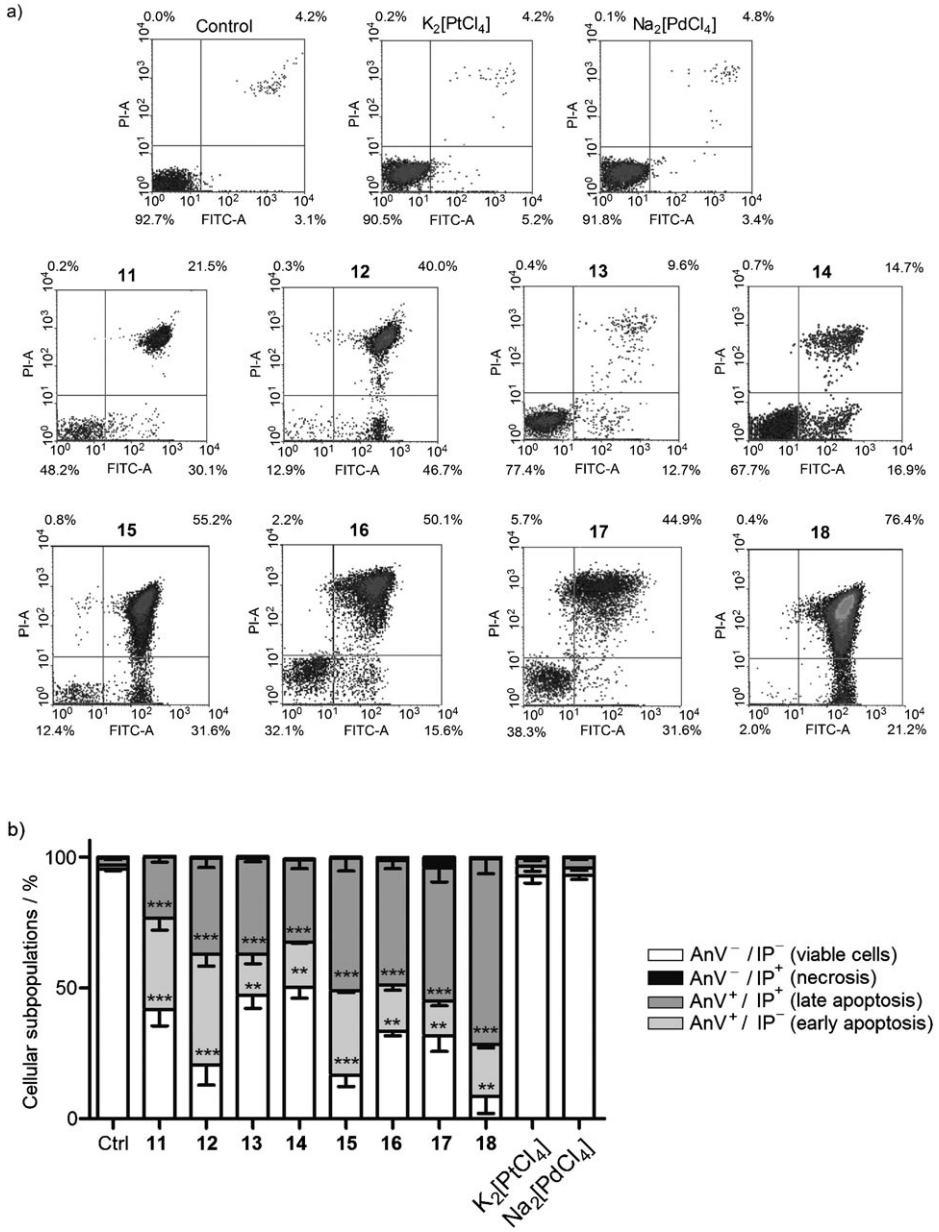

Figure 3. Annexin V assay. Cells were treated for 24 h with: **11**–**14** and $K_2[PtCl_4]$ (20 μM), and **15**–**18** and $Na_2[PdCl_4]$ (0.3 μM). After treatment, the cells were further analyzed as detailed in the Experimental Section. a) Density plots obtained by evaluation with FITC-labeled annexin V (AnV) and propidium iodide (PI). Numbers shown on the density plot refer to the percentage of cells undergoing early stages of apoptosis (lower right quadrant: AnV^+/PI^-), later stages of apoptosis (upper right quadrant: AnV^+/PI^+) and necrosis (upper right quadrant: AnV^-/PI^+). b) Annexin V binding assay. Percentage of cellular subpopulations after treatment with different agents. Data represent the mean ± SEM ($n=3$): (**) $p<0.01$ and (***) $p<0.001$.

bazones exhibit selective apoptotic activity in U937 cells without displaying potential hepatotoxicity, as supported by studies in HepG2 cells. Although palladium(II) complexes derived from 1-indanone thiosemicarbazones were more toxic than platinum(II) derivatives, they were less selective. Platinum(II) complexes selectively enhanced apoptosis in U937 cells suggesting that these compounds may represent promising compounds for the development of novel, selective cytotoxic antileukemia drugs.

Experimental Section

Chemistry

General methods: Elemental analyses were performed on a Carlo Erba Model EA1108 elemental analyzer. Thermogravimetric measurements were performed on a Shimadzu TGA 50 thermobalance with a platinum cell, working under a flow of nitrogen (50 mL min^{-1}) and at a heating rate of 0.5 °C min^{-1} (RT–80 °C) and 1.0 °C min^{-1} (80–350 °C). Conductimetric studies were performed at 25 °C in 10^{-3} M solutions of dimethylformamide (DMF) using a Conductivity Meter 4310 Jenway.[33] Fourier transform infrared (FTIR) spectra (4000–400 cm^{-1}) of the complexes and free ligands were measured as KBr pellets or in Nujol mull with a Bomen FTIR spectrometer (M102 model). The experimental molecular weights (*m/z*) of the free ligands were determined by high-resolution mass spectrometry (HRMS) on a micrOTOF-Q II spectrometer (Bruker Daltonics, Germany) using electrospray ionization (ESI). ESI-MS spectra of the complexes were measured in MeOH with an Esquire 6000 instrument (Bruker Daltonics). Spectra were recorded in the positive mode (105–1000 *m/z*) under the following conditions: end plate offset voltage −500 V, capillary voltage −3500 V, capillary exit 124.0 V, nebulizer 15 psi, dry gas flow 5.00 L min^{-1}, and dry gas temperature 325 °C. ^1H NMR and ^{13}C NMR spectra were obtained in [D_6]DMSO (Sigma) solutions at RT on a Bruker 500 spectrometer, at 500 MHz and 125 MHz, respectively.

The free ligands were prepared and characterized as previously described by condensation of 1-indanones with the appropriate thiosemicarbazide.[5] Both reagents were purchased from Sigma Chemical Co., St. Louis, MO (USA).

Preparation of thiosemicarbazones 1–10: Compounds **1**–**10** were obtained from the corresponding commercial or synthetic 1-indanones combined with thiosemicarbazide or 4-allylthiosemicarbazide. A suspension of the appropriate 1-indanone (1.2 mmol) and the corresponding thiosemicarbazide (2.7 mmol) in abs EtOH (20 mL) was heated under reflux for 30 min. Concd H_2SO_4 (0.10 mL) was then added and heating continued until the 1-indanone starting material was consumed, as indicated by thin-layer chromatography (TLC; silica gel 60 F_{254}; $CHCl_3$/EtOH, 1:0.1). The solvent was

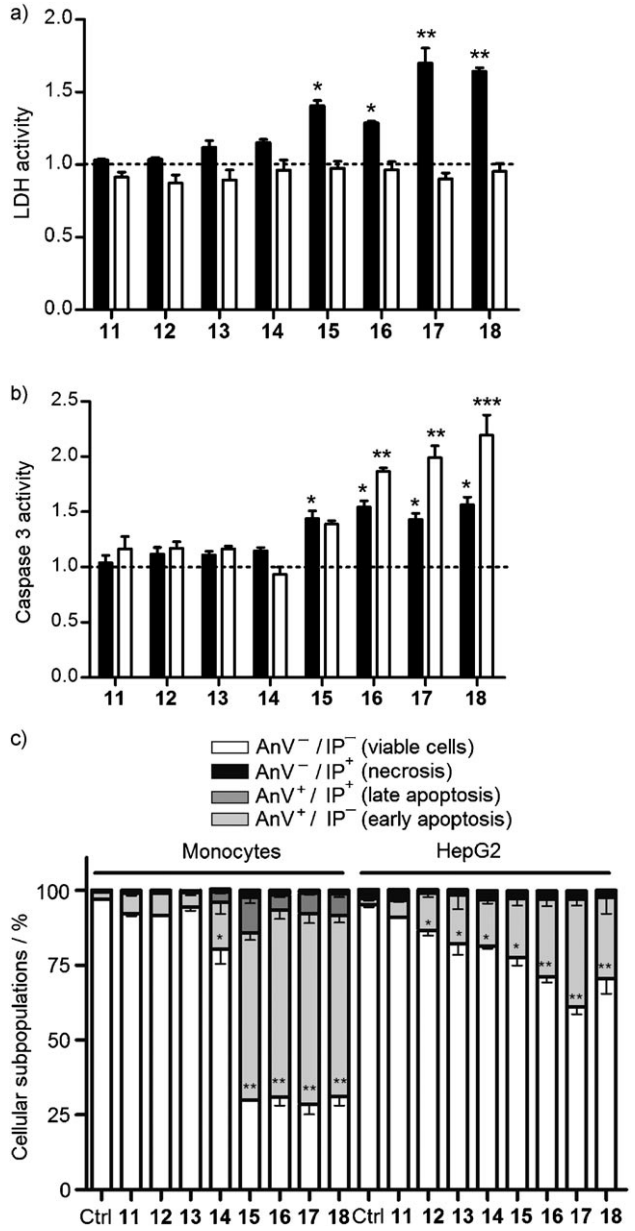

Figure 4. Compound selectivity assessed in normal peripheral blood monocytes (■) and human hepatocellular (HepG2) carcinoma cells (□). Cells were exposed for 24 h to **11**–**14** (20 μM) and **15**–**18** (0.3 μM). After the incubation period was complete, the cells were further analyzed as detailed in the Experimental Section. a) LDH activity with respect to control cells (-----). b) Casapase 3 activity with respect to control cells (-----). c) Annexin V binding assay. Percentage of cellular subpopulations after treatment with different agents. Data represent the mean ± SEM ($n=3$): (*) $p<0.05$, (**) $p<0.01$ and (***) $p<0.001$.

removed in vacuo, and the solid was resuspended in H_2O (20 mL), filtered and washed with H_2O (2×5 mL), EtOH (5 mL), CH_2Cl_2 (5 mL) and hexane (2×5 mL). The identity of compounds **1**–**8** was confirmed by comparison of their physical and spectral data (^{1}H and ^{13}C NMR and IR) with those previously reported.[5]

5-Methoxy-1-indanone-(*N*4-allylthiosemicarbazone) (9): White solid (234 mg, 85%): mp: 144–145 °C; ^{1}H NMR (500 MHz, [D$_6$]DMSO): $\delta=2.87$ (m, 2H), 3.01 (m, 2H), 3.78 (3H, s), 4.21 (t, $J=$ 5.7 Hz, 1H), 5.08 (dd, $J=10.1$, 1.5 Hz, 1H), 5.14 (dd, $J=17.1$, 1.5 Hz, 1H), 5.91 (m, 1H), 6.87 (dd, $J=8.5$, 2.3 Hz , 1H), 6.93 (d, $J=1.8$ Hz, 1H), 7.78 (d, $J=8.4$, 1H), 8.54 (t, $J=5.8$ Hz, 1H), 10.18 ppm (1H, s); ^{13}C NMR (125 MHz, [D$_6$]DMSO): $\delta=28.0$, 28.8, 46.2, 55.9, 110.0, 114.9, 116.0, 123.5, 135.7, 151.4, 157.4, 162.3, 178.0 ppm; IR (Nujol): $\tilde{\nu}=3183$ (NH); 1601 (C=N), 1531 (C(*S*)–N), 841 cm^{-1} (C=S); HRMS (ESI+): *m/z* $[M+H]^+$ calcd for $C_{14}H_{18}N_3OS$: 276.1165, found: 276.1169.

6-Methoxy-1-indanone-(*N*4-allylthiosemicarbazone) (10): White solid (234 mg, 85%): mp: 126–127 °C; ^{1}H NMR (500 MHz, [D$_6$]DMSO): $\delta=2.88$ (m, 2H), 2.96 (m, 2H), 3.79 (3H, s), 4.25 (t, $J=$ 5.7 Hz, 2H), 5.09 (dd, $J=10.3$, 1.4 Hz, 1H), 5.15 (dd, $J=17.2$, 1.4 Hz, 1H), 5.92 (m, 1H), 6.97 (dd, $J=8.2$, 2.5 Hz, 1H), 7.26 (d, $J=8.4$ Hz, 1H), 7.43 (d, $J=2.2$ Hz, 1H), 8.67 (t, $J=5.8$ Hz, 1H), 10.27 ppm (s, 1H); ^{13}C NMR (125 MHz, [D$_6$]DMSO): $\delta=27.9$, 28.4, 46.2, 56.0, 105.8, 115.9, 118.7, 126.7, 135.7, 139.5, 141.4, 157.3, 159.3, 178.2 ppm; IR (Nujol): $\tilde{\nu}=3348$ (NH), 1610 (C=N), 1527 C(*S*)–N, 826 cm^{-1} (C=S); HRMS (ESI+): *m/z* $[M+H]^+$ calcd for $C_{14}H_{18}N_3OS$: 276.11651, found: 276.11731.

Preparation of [MCl$_2$(HL)] (M = Pt or Pd): $K_2[PtCl_4]$ (54 mg, 0.13 mmol) or $Na_2[PdCl_4]$ (38 mg, 0.13 mmol) and the appropriate ligand (0.13 mmol) were heated under reflux in MeOH (10 mL) for 6 h. The resulting solid residue was filtered off and washed with warm H_2O followed by hot MeOH. Solids were dried at room temperature under silica.

[PtCl$_2$(HL1)] (11): Dark yellow solid (35 mg, 58%): IR (KBr): $\tilde{\nu}=1608$ (C=N), 802 cm^{-1} (C=S); Anal. calcd for $C_{10}H_{11}Cl_2N_3PtS$: C 25.5, H 2.35, N 8.92, S 6.80, found: C 25.6, H 2.35, N 8.90, S 6.74; Λ_M (DMF): 11 ohm^{-1} cm^2 mol^{-1}.

[PtCl$_2$(HL2)] (12): Dark yellow solid (31 mg, 48%): IR (KBr): $\tilde{\nu}=1606$ (C=N), 843 cm^{-1} (C=S); Anal. calcd for $C_{12}H_{15}Cl_2N_3O_2PtS$: C 25.5, H 2.35, N 8.92, S 6.80, found: C 25.6, H 2.35, N 8.90, S 6.74; Λ_M (DMF): 10 ohm^{-1} cm^2 mol^{-1}.

[PdCl$_2$(HL1)] (15): Orange–brown solid (25 mg, 51%): IR (KBr): $\tilde{\nu}=$ 1618 (C=N), 815 cm^{-1} (C=S); Anal. calcd for $C_{10}H_{11}Cl_2N_3PdS$: C 31.4, H 2.90, N 11.0, S 8.39, found: C 31.3, H 2.85, N 10.91, S 8.31; Λ_M (DMF): 12 ohm^{-1} cm^2 mol^{-1}.

[PdCl$_2$(HL2)] (16): Orange–brown solid (29 mg, 55%): IR (KBr): $\tilde{\nu}=$ 1605 (C=N), 847 cm^{-1} (C=S); Anal. calcd for $C_{12}H_{15}Cl_2N_3O_2PdS$: C 32.6, H 3.42, N 9.49, S 7.24, found: C 32.5, H 3.39, N 9.42, S 7.22; Λ_M (DMF): 10 ohm^{-1} cm^2 mol^{-1}.

Preparation of [M(HL)(L)]Cl (M = Pt or Pd): $K_2[PtCl_4]$ (54 mg, 0.13 mmol) or $Na_2[PdCl_4]$ (38 mg, 0.13 mmol) and the corresponding ligand (0.26 mmol) were heated under reflux in MeOH (10 mL) for 6 h. The solid was filtered off and washed with warm H_2O followed by hot MeOH. In the case of the Pd compounds, the reflux period was extended to 24 h. The small amount of solid obtained after heating was discarded and the solvent was slowly evaporated over 3–4 days. The solid obtained after partial evaporation of the solvent was filtered off and washed with hot MeOH followed by warm H_2O. Solids were dried at room temperature under silica.

***cis*-[Pt(HL1)(L1)]Cl·CH$_3$OH (13)**: Yellow solid (34 mg, 43%): IR (KBr): $\tilde{\nu}=1609$ (C=N), 802 cm^{-1} (C=S); Anal. calcd for $C_{21}H_{25}ClN_6OPtS_2$: C 37.5, H 3.75, N 12.5, S 9.54, found: C 37.4, H 3.70, N 12.4, S 9.60; MS (ESI+): *m/z* (%): 604.0 $[M]^+$ (100%); Λ_M (DMF): 79 ohm^{-1} cm^2 mol^{-1}. Single crystals of [Pt(HL1)(L1)]Cl·2CH$_3$OH were

obtained by slow evaporation of the solvent: Anal. calcd for $C_{22}H_{29}ClN_6O_2PtS_2$: C 37.5, H 4.15, N 11.93, S 9.11, found: C 37.5, H 4.10, N 11.88, S 9.08.

[Pt(HL2)(L2)]Cl·2H$_2$O (14): Yellow solid (46 mg, 45%): IR (KBr): $\tilde{\nu}$ = 1604 (C=N), 841 cm^{-1} (C=S); Anal. calcd for $C_{24}H_{33}ClN_6O_6PtS_2$: C 36.2, H 4.18, N 10.5, S 8.05, found: C 36.4, H 4.20, N 10.6, S 8.10; MS (ESI+): *m/z* (%): 724.1 $[M]^+$ (100%); Λ_M (DMF): 59 ohm^{-1} cm^2 mol^{-1}.

[Pd(HL1)(L1)]Cl·CH$_3$OH (17): Orange solid (27 mg, 35%): IR (KBr): $\tilde{\nu}$ = 1618 (C=N), 803 cm^{-1} (C=S); Anal. calcd for $C_{21}H_{25}ClN_6OPdS_2$: C 43.2, H 4.32, N 14.4, S 11.0, found: C 43.3, H 4.40, N 14.3, S 10.84; MS (ESI+): *m/z* (%): 515.0 $[M]^+$ (100%); Λ_M (DMF): 60 ohm^{-1} cm^2 mol^{-1}.

[Pd(HL2)(L2)]Cl·2H$_2$O (18): Red–orange solid (27 mg, 30%): IR (KBr): $\tilde{\nu}$ = 1601 (C=N), 848 cm^{-1} (C=S); Anal. calcd for $C_{24}H_{33}ClN_6O_6PdS_2$: C 40.7, H 4.70, N 11.9, S 9.06, found: C 40.9, H 4.71, N 12.0, S 9.15; MS (ESI+): *m/z* (%): 635.0 $[M]^+$ (100%); Λ_M (DMF): 65 ohm^{-1} cm^2 mol^{-1}.

X-ray crystallography

CCDC-778905 contains the supplementary crystallographic data for this paper. These data can be obtained free of charge from The Cambridge Crystallographic Data Centre (CCDC) via www.ccdc.cam.ac.uk. Information concerning crystallographic data collection and structure refinements is summarized in table S1 in Supporting information.

Crystals of dimensions 0.20×0.22×0.30 mm^3 were mounted on a Rigaku AFC-7S automatic four-circle diffractometer and used for data collection. Diffraction data were acquired at RT by graphite monochromated Mo–Kα radiation (λ = 0.71069 Å) with the $\omega-2\theta$ scan mode. The unit cell parameters were determined from least-squares refinement of the setting angles of 25 reflections in the 2θ ranges 25–30°. Examination of three standard reflections, monitored after every 150 reflections, showed signs of rapid crystal deterioration with intensity loss of 70% during data collection up to 2θ = 50°. Intensity decay, Lorentz polarization and ψ-scan absorption corrections (MSC/AFC Diffractometer Software, 1993) were applied to the intensity data. All nonhydrogen atoms were refined anisotropically, and all hydrogen atoms were included in the model in geometrically suitable positions and refined riding with $U_{iso} = 1.2U_{eq}$ of the parent atom except for methanol hydrogens where $U_{iso} = 1.5U_{eq}$ of the parent atom was used. The refinement was performed on F^2 against 4344 observed reflections using seven geometrical or thermal parameters restraints. The maximum and minimum values of the electron density found in the final Fourier-difference maps were 4.63 and −3.81 e Å^{-3}. Maximum or minimum peaks were found less than 1 Å far from the platinum atom. The decomposition of the crystals studied, evidenced by the high decay of the intensity of the standard reflections, also led to low quality data producing high residuals and low accuracy in the final parameters. The structure was solved by the Patterson method and subsequently completed automatically by Fourier recycling using DIRDIF[34] achieving the determination of coordinates for more than 80% of the atoms in the structure. Structural completion and refinement were performed with the SHELX-97 package running under WinGX suite of programs.[35,36] The final geometrical calculations were performed using the PLATON program.[37]

Biological studies

Cell culture: The human histiocytic lymphoma U937 cell line (American Type Culture Collection, Rockville, MD, USA) was cultured at 37 °C in a humidified 5% CO_2 atmosphere in RPMI 1640 medium (Sigma–Aldrich), supplemented with 10% fetal calf serum (FCS) and 50 μg mL^{-1} gentamicin. The human hepatocellular carcinoma HepG2 cell line (American Type Culture Collection) was grown at 37 °C in a humidified atmosphere with 5% CO_2 in Dulbecco's modified eagle's medium (Sigma–Aldrich), supplemented with 10% FCS and 50 μg mL^{-1} gentamicin. HepG2 cells were plated 24 h before each assay.

Peripheral blood monocytes were isolated from healthy volunteers by standard density gradient centrifugation on Ficoll–Hypaque. Monocytes were purified by centrifugation on a discontinuous Percoll gradient as previously described with minor modifications.[38] Briefly, peripheral blood monocytes were suspended in Ca_2^+- and Mg^{2+}-free Tyrode solution supplemented with 0.2% ethylenediaminetetraacetic acid (EDTA) and incubated for 30 min at 37 °C. The medium osmolarity was gradually increased from 290 to 360 Osmol L^{-1} by the addition of 9% aq NaCl solution. Three different Percoll fractions were layered in polypropylene tubes: 50% at the bottom followed by 46% and 40%. The top peripheral blood monocyte (5.10×106 mL) layer was centrifuged at 400 *g* for 20 min at 4 °C. Monocytes were recovered at the 50–46% interface. Purity was checked by FACS analysis using anti-CD14 monoclonal antibodies and was found to be >85%. Cells were cultured at 37 °C in a humidified atmosphere with 5% CO_2 in RPMI 1640 medium, supplemented with 10% FCS and 50 μg mL^{-1} gentamicin. Before seeding, the viability of U937 cells, HepG2 cells and monocytes was tested by Trypan blue assay. Cells were used if viability was greater than 90%.

Cell growth inhibition assay: U937 cells growing in exponential phase were seeded at 2.0×10^4 cells in 200 μL RPMI 1640 in a 96-well culture plate and incubated under a 5% CO_2 atmosphere. Cells were exposed for 48 h to different concentrations of the compounds: 0.78–50 μM for compounds **1**–**14** and K_2PtCl_4; 0.039–2.5 μM for compounds **15**–**18** and $Na_2[PdCl_4]$, followed by incubation with 0.5 μCi of [^{3}H]methylthymidine (PerkinElmer, Boston, MA, USA), added 12 h before the end of the experiment. The cells were then harvested using an automatic cell harvester (Nunc, Maryland, USA). The incorporation of the radioactive nucleotide was measured in a Pharmacia Wallac 1410 liquid scintillation counter and expressed as incorporation percentage with respect to a control group (cells grown in culture medium). IC_{50} values were calculated by the equation for sigmoidal dose–response using Prism 5.00 for Windows (GraphPad Software, San Diego, CA, USA). Assays were performed in triplicate and at least three independent experiments were conducted.

Cytotoxic activity determination: Cells growing in exponential phase were seeded at 3.5×10^4 cells in 200 μL RPMI 1640 in a 48-well culture plate and incubated under a 5% CO_2 atmosphere for 48 h. Cells were exposed at different compound concentrations: 0.78–50 μM for compounds **1**–**14** and K_2PtCl_4; 0.039–2.5 μM for compounds **15**–**18** and $Na_2[PdCl_4]$. Following incubation, 20 μL 0.4% trypan blue was added and viable cells were estimated by a hemocytometer chamber. CC_{50} values were calculated using the equation for sigmoidal dose–response using Prism 5.00 for Windows (GraphPad Software). Assays were carried out in duplicate and at least three independent experiments were conducted.

Following cell exposure at the IC_{50} value of the different derivatives, the cytotoxic activity was assessed by lactate dehidrogenase (LDH) release. Cells growing at exponential phase were seeded at 3.5×10^4 in 200 μL of culture medium in a 48-well plate and were incubated for 24 h either with medium alone or with 20 μM compounds **11**–**14** or 0.3 μM compounds **15**–**18**. At the end of the incubation, LDH release was determined using a CytoTox 96 non-radioactive cytotoxicity assay kit (Promega).

Determination of cleaved caspase 3 and PARP by Western blot analysis: Following 24 h exposure to the IC_{50} value of the different compounds, cells were lysed in 50 mM Tris-HCl pH 6.8, 2% sodium dodecyl sulfate (SDS), 100 mM 2-mercaptoethanol, 10% glycerol and 0.05% bromophenol blue and sonicated to shear DNA. Total cell lysates were resolved by SDS-PAGE, immunoblotted with anti-caspase 3 rabbit polyclonal antibody or with anti-poly (ADP-ribose) polymerase (PARP) rabbit antibody (Santa Cruz Biotechnology, CA, USA) followed by horseradish peroxidase conjugated anti-rabbit IgG (Santa Cruz Biotechnology), and developed by enhanced chemiluminesence (ECL) following the manufacturer's instructions (Amersham Life Science, Amersham Place, Little Chalfont Buckinghamshire, England).

Caspase 3 enzymatic activity assay: Cells growing in exponential phase were treated for 24 h with 20 μM compounds **11**–**14**, 0.3 μM compounds **15**–**18**. Cells were then harvested and processed according to CASP3C caspase 3 colorimetric assay kit (Sigma Chemical Co., St. Louis, MO, USA).

Annexin V binding assay: Cells growing in exponential phase were exposed for 24 h to 20 μM compounds **11**–**14**, 0.3 μM compounds **15**–**18**. After washing with cold phosphate-buffered saline, 2.0×10^5 cells were incubated with fluorescein isothiocyanate (FITC)-labeled annexin V and propidium iodide (annexin V-FITC assay kit, Invitrogen) and analyzed on a FACS scan flow cytometer (Becton–Dickinson, Frankling Lakes, NJ, USA).

Statistical analysis: IC_{50} and CC_{50} values were calculated by the equation for sigmoidal dose–response using software Prism 5.00 for Windows (GraphPad Software). Logarithmic transformation of the variable was required prior one-way ANOVA followed by the Student Newman–Keuls test (GraphPad InStat version 3.01), where $p < 0.05$ was considered statistically significant.

Acknowledgements

D.S. thanks ANII-Uruguay for a research grant (BE 2008 230). This work was financially supported by the Agencia Nacional de Promoción Científica y Tecnología (PICT 07–01725), the Universidad de Buenos Aires (Argentina) (UBACyT B033), and the Prosul-CNPq (Uruguay) (Proc. 490.600/2007–8). The authors thank Dr. Alejandra Rodríguez and Natalia Berta Rossi (Química Analítica, Polo Tecnológico, Facultad de Química, Uruguay) for performing the mass spectrometry of the metal complexes, and Dr. Eugenia Riveiro for her invaluable technical assistance. This work was made possible by fellowships awarded by the Consejo Nacional de Investigaciones Científicas y Técnicas (CONICET) (Argentina).

Keywords: apoptosis · drug discovery · leukemia · metal complexes · thiosemicarbazones

[1] M. Leszczyniecka, T. Roberts, P. Dent, S. Grant, P. B. Fisher, *Pharmacol. Ther.* **2001**, *90*, 105–156.
[2] S. H. Kaufmann, *Cancer Res.* **1989**, *49*, 5870–5878.
[3] C. C. García, B. N. Brousse, M. J. Carlucci, A. G. Moglioni, M. Martins Alho, G. Y. Moltrasio, N. B. D'Accorso, E. B. Damonte, *Antiviral Chem. Chemother.* **2003**, *14*, 99–105.
[4] B. N. Brousse, R. Massa, A. G. Moglioni, M. Martins Alho, N. D'Accorso, G. Gutkind, G. Y. Moltrasio, *J. Chil. Chem. Soc.* **2004**, *49*, 45–45.
[5] L. M. Finkielsztein, E. F. Castro, L. E. Fabian, G. Y. Moltrasio, R. H. Campos, L. Cavallaro, A. G. Moglioni, *Eur. J. Med. Chem.* **2008**, *43*, 1767–1773.
[6] R. A. Finch, M. Liu, S. P. Grill, W. C. Rose, R. Loomis, K. M. Vasquez, Y. Cheng, A. C. Sartorelli, *Biochem. Pharmacol.* **2000**, *59*, 983–991.
[7] H. Beraldo, D. Gambino, *Mini-Rev. Med. Chem.* **2004**, *4*, 31–39.
[8] Y. Yu, D. S. Kalinowski, Z. Kovacevic, A. R. Siafakas, P. J. Jansson, C. Stefani, D. B. Lovejoy, P. C. Sharpe, P. V. Bernhardt, D. R. Richardson, *J. Med. Chem.* **2009**, *52*, 5271–5294.
[9] D. S. Kalinowski, D. R. Richardson, *Pharmacol. Rev.* **2005**, *57*, 547–583.
[10] B. Ma, B. C. Goh, E. H. Tan, K. C. Lam, R. Soo, S. S. Leong, L. Z. Wang, F. Mo, A. T. Chan, B. Zee, T. Mok, *Invest. New Drugs* **2008**, *26*, 169–173.
[11] A. M. Traynor, J. W. Lee, G. K. Bayer, J. M. Tate, S. P. Thomas, M. Mazurczak, D. L. Graham, J. M. Kolesar, J. H. Schiller, *Invest. New Drugs* **2010**, *28*, 91–97.
[12] P. Tarasconi, S. Capacchi, G. Pelosi, M. Cornia, R. Albertini, A. Bonati, P. P. Dall'Aglio, P. Lunghi, S. Pinelli, *Bioorg. Med. Chem.* **2000**, *8*, 157–162.
[13] A. P. da Silva, M. V. Martini, C. M. de Oliveira, S. Cunha, J. E. de Carvalho, A. L. Ruiz, C. C. da Silva, *Eur. J. Med. Chem.* **2010**, *45*, 2987–2993.
[14] D. R. Richardson, P. C. Sharpe, D. B. Lovejoy, D. Senaratne, D. S. Kalinowski, M. Islam, P. V. Bernhardt, *J. Med. Chem.* **2006**, *49*, 6510–6521.
[15] A. Buschini, S. Pinelli, C. Pellacani, F. Giordani, M. B. Ferrari, F. Bisceglie, M. Giannetto, G. Pelosi, P. Tarasconi, *J. Inorg. Biochem.* **2009**, *103*, 666–677.
[16] P. J. Jansson, P. C. Sharpe, P. V. Bernhardt, D. R. Richardson, *J. Med. Chem.* **2010**, *53*, 5759–5769.
[17] D. C. Reis, M. C. Pinto, E. M. Souza-Fagundes, S. M. Wardell, J. L. Wardell, H. Beraldo, *Eur. J. Med. Chem.* **2010**, *45*, 3904–3910.
[18] M. Vieites, L. Otero, D. Santos, C. Olea-Azar, E. Norambuena, G. Aguirre, H. Cerecetto, M. Gonzalez, U. Kemmerling, A. Morello, J. Diego Maya, D. Gambino, *J. Inorg. Biochem.* **2009**, *103*, 411–418.
[19] M. Vieites, L. Otero, D. Santos, J. Toloza, R. Figueroa, E. Norambuena, C. Olea-Azar, G. Aguirre, H. Cerecetto, M. Gonzalez, A. Morello, J. D. Maya, B. Garat, D. Gambino, *J. Inorg. Biochem.* **2008**, *102*, 1033–1043.
[20] L. Otero, M. Vieites, L. Boiani, A. Denicola, C. Rigol, L. Opazo, C. Olea-Azar, J. D. Maya, A. Morello, R. L. Krauth-Siegel, O. E. Piro, E. Castellano, M. Gonzalez, D. Gambino, H. Cerecetto, *J. Med. Chem.* **2006**, *49*, 3322–3331.
[21] A. I. Matesanz, P. Souza, *Mini-Rev. Med. Chem.* **2009**, *9*, 1389–1396.
[22] D. Gambino, L. Otero, M. Vieites, M. Boiani, M. González, E. J. Baran, H. Cerecetto, *Spectrochim. Acta, Part A* **2007**, *68*, 341–348.
[23] D. Kovala-Demertzi, J. R. Miller, N. Kourkoumelis, S. K. Hadjikakou, M. A. Demertzis, *Polyhedron* **1999**, *18*, 1005–1013.
[24] D. Kovala-Demertzi, A. Domopoulou, M. Demertzis, C. P. Raptopoulou, A. Terzis, *Polyhedron* **1994**, *13*, 1917–1925.
[25] L. M. Fostiak, I. García, J. K. Swearingen, E. Bermejo, A. Castiñeiras, D. X. West, *Polyhedron* **2003**, *22*, 83–92.
[26] J. S. Casas, E. E. Castellano, J. Ellena, M. S. Garcia-Tasende, M. L. Perez-Paralle, A. Sanchez, A. Sanchez-Gonzalez, J. Sordo, A. Touceda, *J. Inorg. Biochem.* **2008**, *102*, 33–45.
[27] R. J. Glisoni, D. A. Chiappetta, L. M. Finkielsztein, A. G. Moglioni, A. Sosnik, *New J. Chem.* **2010**, *34*, 2047–2058.
[28] D. Kanduc, A. Mittelman, R. Serpico, E. Sinigaglia, A. A. Sinha, C. Natale, R. Santacroce, M. G. Di Corcia, A. Lucchese, L. Dini, P. Pani, S. Santacroce, S. Simone, R. Bucci, E. Farber, *Int. J. Oncol.* **2002**, *21*, 165–170.
[29] K. Stahnke, S. Eckhoff, A. Mohr, L. H. Meyer, K. M. Debatin, *Leukemia* **2003**, *17*, 2130–2139.
[30] A. Gómez Quiroga, C. Navarro Ranninger, *Coord. Chem. Rev.* **2004**, *248*, 119–133.

[31] Y. Yoshida, N. Anzai, H. Kawabata, *Crit. Rev. Oncol. Hematol.* **1996**, *24*, 185 – 211.
[32] K. S. Ferraz, L. Ferandes, D. Carrilho, M. C. Pinto, M. F. Leite, E. M. Souza-Fagundes, N. L. Speziali, I. C. Mendes, H. Beraldo, *Bioorg. Med. Chem.* **2009**, *17*, 7138 – 7144.
[33] W. J. Geary, *Coord. Chem. Rev.* **1971**, *7*, 81 – 122.
[34] P. T. Beurskens, G. Beurskens, R. de Gelder, S. Garcia-Granda, R. O. Gould, R. Israel J. M. M. Smits, The DIRDIF-99 program system, Crystallography Laboratory, University of Nijmegen (The Netherlands), **1999**.
[35] G. M. Sheldrick, SHELXL97, Program for Structure Refinement, University of Göttingen (Germany), **1997**.
[36] L. J. Farrugia, *J. Appl. Crystallogr.* **1999**, *32*, 837 – 838.
[37] A. Spek, L. A. Platon, Multipurpose Crystallographic Tool, Utrecht University, Utrecht (The Netherlands), **2003**.
[38] H. E. Chuluyan, A. C. Issekutz, *J. Clin. Invest.* **1993**, *92*, 2768 – 2777.

Received: February 4, 2011
Revised: April 26, 2011
Published online on May 23, 2011

